Self-Pulsating Semiconductor Lasers: Theory and Experiment

- C. R. Mirasso¹, G.H.M. van Tartwijk^{2,*}, E. Hernández-García^{3,1}, D. Lenstra², S. Lynch⁴, P. Landais⁴, P. Phelan ⁵, J. O'Gorman⁴, M. San Miguel^{3,1}, and W. Elsäßer⁶
- ¹ Departament de Física, Universitat de les Illes Balears, E-07071 Palma de Mallorca, Spain.
 - ² Department of Physics and Astronomy, Vrije Universiteit, De Boelelaan 1081, 1081 HV Amsterdam, The Netherlands.
 - ³ Instituto Mediterraneo de Estudios Avanzados IMEDEA, CSIC-UIB, E-07071 Palma de Mallorca, Spain.
 - ⁴ Optronics Ireland, Physics Department, Trinity College, Dublin 2, Republic of Ireland.
 - ⁵ Physics Department, Trinity College, Dublin 2, Republic of Ireland.
- ⁶ Institut für Angewandte Physik, Technische Universität Darmstadt, Schloßgartenstraße 7, 62289 Darmstadt, Germany.
 - * Present address: Philips Optoelectronics B.V, Prof. Holstlaan 4, 5656 AA Eindhoven,
 The Netherlands

(Published in IEEE J. Quantum Electron. 35, 764-770 (1999).)

Abstract

We report detailed measurements of the pump-current dependency of the self-pulsating frequency of semiconductor CD lasers. A distinct kink in this dependence is found and explained using rate-equation model. The kink denotes a transition between a region where the self-pulsations are weakly sustained relaxation oscillations and a region where Q-switching takes place. Simulations show that spontaneous emission noise plays a crucial role for the cross-over.

I. INTRODUCTION

Self-pulsating semiconductor lasers (SPSL's) are of great interest owing to their potential application in telecommunication systems as well as in optical data storage applications. In particular, in the latter case they are realized as so-called narrow–stripe geometry CD lasers where the self-pulsation is achieved via saturable absorption in the transverse dimension limiting the active region. A profound knowledge and understanding of their operation dynamics is therefore desired.

SPSL's have been studied since the first diode lasers became available in the late 1960s [1]. These first semiconductor lasers, although designed to operate in continuous wave (CW) mode, showed self-induced pulsations of the light intensity due to a combination of two reasons: (i) the laser resonance is internally excited through the nonlinear interaction of various longitudinal laser modes, thus causing mode beating at very high frequency; (ii) defects in the active material act as saturable absorbing areas, thus causing absorptive Q-switching processes.

In the case of self-pulsations caused by saturable-absorbing effects, the self-pulsation frequency (SPF) dependence on the pump current was investigated in [2]. In later works the self pulsations were attributed to undamped relaxation oscillations (RO) [3,4]. The precise values of the ROF, as calculated from a small-signal analysis, and the actual SPF, highly nonlinear, are however different, the SPF being always smaller than the ROF [5].

Saturable absorption effects, causing self-pulsations in stripe-geometry lasers have been investigated since the early 1980s [6–8]. Saturable absorption is also responsible for self-pulsations in double-section laser diodes [9]. A similar mechanism of dispersive Q-switching has been invoked to describe self-pulsations in multisection Distributed Feedback Lasers [10–12].

In this paper we study both experimentally and theoretically the dependence of the selfpulsation frequency (SPF) of narrow–stripe geometry self-pulsating semiconductor lasers, also known as CD–lasers, on the bias pump current. In these lasers, self–pulsation is induced via saturable absorption in the transverse dimension of the active region. The rate—equation model of Ref. [3] has been proven to be quite successful in describing the mechanism of self-pulsation and has already been used with success in analyzing such lasers subject to weak optical feedback [5]. There it was found that, with and without feedback, there are two distinct regions in the SPF vs. pump—current curve, one where spontaneous emission dominates the laser dynamics between pulses and one where spontaneous emission always plays a minor role.

In section II we present detailed measurements of the SPF vs pump-current curve. This curve confirms most of the findings of [5], and also shows a distinct cross-over point distinguishing between linear and square-root-like behavior. In section III we confront the experimental results with a theoretical model, inspired by Ref. [3]. Its results agree qualitatively well with the experimental results, showing a distinct cross-over region. The location of the cross-over region is shown to be determined by the spontaneous emission rate. In Section IV we discuss the relationship between the SPF and the ROF using a small signal analysis. We discuss the various bifurcations that are predicted by our model, and compare it with the model of Ref. [5].

II. EXPERIMENT

We use a SHARP CD semiconductor laser diode, model LTO22MD. The laser emits a continuous train of regular pulses with a frequency that depends on the bias pump current. A bulk layer of AlGaAs constitutes the active layer of this Fabry-Perot cavity that emits at 800–nm wavelength. The gain section is defined by the p-electrical contact and has the following approximate dimensions: $250-\mu$ m long, $2-\mu$ m wide, and $0.2-\mu$ m thick. A very narrow contact of $\sim 2\mu$ m allows for current injection. Since the region capable of stimulated emission extends to both sides beyond the narrow stripe of the current contact, the wings of the optical field distribution will interact with these unpumped, and therefore absorbing, regions. In fact, these regions are saturably absorbing; when the optical intensity in the

wings of the mode is large enough, the electron-hole pair population in the unpumped region reaches transparency, thus allowing a "self-Q-switched" pulse. There is no sharp boundary between the pumped and unpumped regions, making carrier diffusion an important effect. Indeed, in the model of Ref. [3] carrier diffusion between the pumped and unpumped regions is crucial for the appearance of self-pulsation.

The experimental set-up is illustrated in Fig. 1. The laser is temperature controlled by a Peltier cooler at 20 C. It is DC biased by a low noise current supply. Laser emission is collected by an anti-reflection coated 0.65 N.A. laser diode lens. The resulting parallel beam is passed through a 30–dB isolator to avoid spurious effects caused by optical feedback and is launched into a 60–GHz photodiode (New Focus Model 1006). The converted electrical signal is observed with a 22–GHz bandwidth spectrum analyzer (HP 8563A). The typical RF spectrum of the SPSL is characterized by a main peak at the SPF, followed by overtones. The uncertainty on the self-pulsation frequency measurement is mainly due to the measurement of bias current, which has an error of less than 0.1 mA. The resolution of the spectrum analyzer is 100 kHz and the video filter is 30 kHz.

For values near the threshold current, the low power emission makes it difficult to observe the signal. The value of the spectral density of the self pulsations is very close to the noise level and also the width of the feature in the power spectrum is wider than at higher currents. To overcome this problem, a small current modulation is applied to the device for injection currents below 47 mA [13], [14]. Its power is kept sufficiently low so that it does not affect the oscillation behaviour of the laser and does not induce any supplementary oscillation phenomena, e.g. relaxation oscillation or self-pulsations originating from a cross modulation of the carrier density. The self-pulsation frequency shows up as an enhancement of the oscillation of the laser emission if the two frequencies coincide. This allows an accurate determination of the SPF frequency close to threshold.

Figure 2 a shows the optical power and SPF as a function of the bias current. The L-I curve has been recorded using an integrating sphere. It is assumed that all emitted power is collected. The laser is characterized by a threshold current of ~ 44 mA and a slope efficiency

of 0.22 mW/mA. The SPF varies from 1 to 4 GHz in a bias current range of 46 to 64 mA, which was the maximum injection current we could reach with these devices. In the region of the lasing threshold the experimental values present a square-root like behavior dependence reminiscent of standard relaxation oscillations as exhibited by a CW-semiconductor laser. For bias currents above 55 mA this dependence was no longer observed and the SP behavior appears to have a more linear dependence on the bias current.

III. THEORY

In this section we use a simple model to explain the observed bias-current dependence of the SPF. The investigated laser has a narrow-stripe geometry, which can be modeled in a straightforward way using rate-equations [3] for the optical intensity S (suitably normalized to represent the number of photons in the cavity), the number of electron-hole pairs N_1 in the pumped region, and the number of electron-hole pairs N_2 in the unpumped (absorbing) region:

$$\frac{dS}{dt} = [g_1(N_1 - N_{t1}) + g_2(N_2 - N_{t2}) - \kappa]S + R_{sp} + F_S(t), \tag{1a}$$

$$\frac{dN_1}{dt} = \frac{J}{e} - \frac{N_1}{\tau_s} - g_1(N_1 - N_{t1})S - \frac{N_1 - vN_2}{T_{12}},\tag{1b}$$

$$\frac{dN_2}{dt} = -\frac{N_2}{\tau_s} - g_2(N_2 - N_{t2})S + \frac{N_1/v - N_2}{T_{21}}.$$
 (1c)

where g_1 (g_2) is the gain coefficient at the transparency number N_{t1} (N_{t2}) in the pumped (unpumped) region, κ is the total loss rate. $R_{sp} = \beta_{sp}\eta_{sp}N_1/\tau_s$ is the spontaneous emission rate, η_{sp} is the spontaneous quantum efficiency, β_{sp} is the spontaneous emission factor and τ_s is the carrier lifetime. $F_S(t)$ is a delta-correlated Langevin noise source [15] with correlation $\langle F_S(t_1)F_S(t_2) \rangle = 2R_{sp}S\delta(t_1-t_2)/\tau_s$, J is the bias pump-current, e is the elementary charge, $v = V_1/V_2$ is the volume ratio of pumped and unpumped region, T_{12} is the diffusion time from the pumped region to the unpumped region, and T_{21} is the diffusion time from unpumped to pumped region. These two diffusion times are interrelated through the volume ratio v [3,5]:

$$v = \frac{V_1}{V_2} = \frac{T_{12}}{T_{21}}. (2)$$

Our model (1a-1c) is a simplification of the model used in Ref. [5], where the carrier dependence of the carrier lifetime τ_s is taken into account using the well-known second order expression for τ_s^{-1} in the carrier number N_j . Here, we neglect this dependence for the moment, as it simplifies the analytical work and qualitatively gives similar results.

Using the parameter values listed in Table 1, Eqs. (1a-1c) are numerically solved with a standard algorithm [5]. In Figure 3 we show the resulting SPF-J curves, with and without spontaneous emission noise. Each value of the curves is calculated from an average over 10^3 pulses. It is seen that the observed kink in the SPF-J curve is the result of spontaneous emission noise. There is a shift of the kink towards larger currents upon increasing the spontaneous emission level. For the values of table 1 and $\beta_{sp} = 1.3 \times 10^{-6}$, $J_{xover} \approx 82$ mA. It should be noticed that we do not expect a quantitave agreement between experimental and numerical results, since the model neglects important effects, such as gain saturation. Nevertheless, the qualitative trends are well reproduced allowing us to physically understand the origin of the experimental features.

Figure 4 shows time traces of the intensity for different bias currents. Clearly, the interpulse intensity drastically increases with current in the vicinity of the kink. For currents $J << J_{xover}$ the interpulse intensity is well dominated by the spontaneous emission (panel a)), while for currents $J > J_{xover}$ spontaneous emission does not affect the intensity significantly. The kink-current J_{xover} can be defined as the highest current at which the interpulse intensity is dominated by spontaneous emission noise. As can be seen in Eq. (1a) spontaneous emission increases the intensity generation rate with an amount R_{sp} . The effect of this on the self-pulsation process depends on the generation rate through stimulated emission $R_{stim} = [g_1(N_1 - N_{t1}) + g_2(N_2 - N_{t2})]S$. For currents $J < J_{xover}$, $R_{sp} > R_{stim}$ in the interpulse region while for $J > J_{xover}$, the contrary happens. Therefore, the kink pump current J_{xover} could be mathematically identified through

$$R_{sp} \equiv R_{stim}(J_{xover}),\tag{3}$$

where the current dependence of R_{stim} reflects the need to solve Eq. (3) implicitly using all three equations (1a-1c) at the time at which the intensity reaches the minimum.

The long-dashed curve in Fig. 3 is obtained by putting $R_{sp} = 0$ in Eq. (1a). In that situation, the interpulse intensity becomes extremely small upon decreasing the pump current. The smaller the interpulse intensity becomes, the longer it takes for the absorber to reach transparency. When including noise $(R_{sp} \neq 0)$, the interpulse intensity remains at a much higher level in the same pump current interval because of the spontaneous emission rate R_{sp} . This will significantly increase the speed with which a new pulse is generated after the previous one has depleted the absorber. We note that the Langevin noise source $F_S(t)$ in Eq. (1a) is responsible for the timing jitter of the pulses. In the region $J < J_{xover}$ a single noise event in between pulses may significantly delay or advance the birth of the next pulse, causing substantial jitter. For pump currents above the cross-over, the relative effect of the noisy events, and hence the jitter, is much smaller. The existence of two pump current regions with very different jitter characteristics was also found in Ref. [5].

In figure 5 the maximum pulse intensity (S_{max}) and the minimum interpulse intensity (S_{min}) vs. the bias current are shown. An abrupt change (note that the scale in panel c) is logarithmic) of S_{min} can be seen at J_{xover} (while S_{max} takes it maximum value). The kink-current J_{xover} is therefore identified as the highest current at which the interpulse intensity is dominated by spontaneous emission noise. The kink also denotes the boundary between two regimes that can be described as follows: For currents larger than J_{xover} the self-pulsation has the character of undamped RO, while for currents below this value clear self-Q-switching takes place. Obviously, for currents $J > J_{xover}$ the absorber is not depleted deeply enough to cause a Q-switch: as soon as transparency is reached, the absorber is bleached but the pump is strong enough to prevent total bleaching. For currents $J < J_{xover}$, the pump is small enough to allow total bleaching of the absorbing regions, after which the number of electron-hole pairs in the absorbing region has to start all over again. No bifurcation in the usual sense can, however, be attributed to this critical current.

In the next section, we will look at the relationship between ROF and SPF in more

detail.

IV. RELAXATION OSCILLATIONS AND SELF-PULSATIONS

In the previous section we introduced a simple model which provides an explanation for the peculiar cross-over region in terms of the average level of spontaneous emission. Here we will put our numerical findings in an analytical framework, which leads to a clearer picture of the self-pulsation characteristics.

This is achieved by solving for the CW solutions of Eqs. (1a-1c) and investigating their stability properties. First we look for laser threshold, which is defined as the circumstance for which the trivial solution (S = 0) looses stability in the absence of spontaneous emission. We therefore put $R_{sp} = 0$ in Eq. (1a) and obtain:

$$N_{th} = \frac{g_1 N_{t1} + g_2 N_{t2} + \kappa}{g_1 + \frac{g_2 \tau_s}{T_{12} + v \tau_s}} \tag{4}$$

$$\frac{J_{th}}{e} = N_{th} \left[\frac{1}{\tau_s} + \frac{1}{T_{12}} - \frac{v}{T_{12}} \frac{\tau_s}{T_{12} + v \tau_s} \right]$$
 (5)

Using the parameters listed in Table 1, we find $J_{th} = 44.53$ mA.

In total, Eqs. (1a-1c) have three possible CW solutions. Below threshold, only the solution with S=0 is physically meaningful (the other two have negative power). At threshold the solution S=0 becomes unstable while one of the other two becomes stable with positive power. This is found after performing a standard linear stability analysis, which yields for every CW solution a set of (complex) characteristic exponents $\lambda = \lambda_r + i\lambda_i$. When any of these exponents has a positive real part $(\lambda_r > 0)$, the CW solution is unstable. The imaginary part λ_i denotes the frequency with which perturbations initially will grow. Figure 6 shows how the real parts of the characteristic exponents of the relevant CW solution vary with bias current. The CW solution is found to be unstable on the interval $44.556 \lesssim J \lesssim 92$ mA. For bias currents J > 92 mA, stable CW emission is found. On the other side of the interval, a more complex behavior is found. At J = 44.53 mA, the CW solution is stable, but looses its stability already at J = 44.556 mA. This sequence of bifurcations from the

nonlasing (S = 0) state to self pulsation occurs in a very narrow range of currents around threshold. Thus the sequence will be experimentally very hard to resolve due to different noise sources; the laser will seemingly begin to oscillate as soon as it crosses threshold.

Thus, our model (1a-1c) shows that there exists a CW solution that looses stability at J=44.556 mA and regains stability at J=92 mA. In between these values, the CW state is unstable, as indicated by a complex conjugate pair of characteristic exponents with positive real parts (Hopf-instability). The region of instability coincides obviously with the region of self-pulsating behavior, and is bounded by two Hopf-bifurcations. When the laser operates at a bias current 44.556 < J < 92 mA, small perturbations to the CW state in question initially grow as $\exp\left[(\lambda_r + i\lambda_i)t\right]$, i.e., with angular frequency λ_i . The linear stability analysis does not provide any information on how this initial growth will saturate. Numerical results from Eqs. (1a-1c) show that the resulting SPF is always smaller than the ROF $\lambda_i/2\pi$. This is illustrated in Fig. 3. Both frequencies meet at J=44.556 mA and at J=92 mA, the two Hopf bifurcation points. In the former case it means that the SPF must increase when coming from higher bias currents to reach the RO value. However, this increase only occurs in a very small range of currents so that it would be very hard to observe in the experiment.

It should be noted that a different scenario is found in Ref. [5]. There, the carrier lifetime τ_s is considered to be carrier dependent, to account for the radiative, non-radiative, and Auger processes [22]:

$$\tau_{s,j}^{-1}(N_j) = A_{nr,j} + B_j N_j + C_j N_j^2, \tag{6}$$

where j = 1 denotes the pumped region and j = 2 denotes the unpumped region. This carrier dependence is considered necessary because during the strong pulsations, large variations in the carrier numbers N_j may occur [22].

It was found in Ref. [5] that the carrier dependence of $\tau_{s,j}(N_j)$ plays a significant role around threshold. This is in sharp contrast with the well-known CW edge-emitting lasers where N is clamped immediately above threshold. The kink region, lying far above threshold, is not affected significantly by taking into account the carrier dependence of τ_s . This

illustrates the robustness of the cross-over behavior. At the high end of the self-pulsation interval, also a Hopf bifurcation is found, but the dynamics at the low end differs from the one discussed here. First of all, there is no window of stability just after threshold. Figure 7 shows the location of the various CW solutions as a function of bias pump current. The S=0 solution (horizontal solid line) is only shown for currents where it is stable. It looses stability at $J=J_{th}$. Around $J=0.85J_{th}$ two CW solutions are born out of a bifurcation. Both CW solutions are linearly unstable. This is in contrast with the model discussed above where the upper branch CW solution is stable in a short pump interval after its birth. The bifurcation which starts the self-pulsation is not a Hopf one but a homoclinic bifurcation (collision of a limit cycle and saddle). Thus, in the model of Ref. [5] self-pulsation occurs in a region bounded by a Hopf-bifurcation on the high bias side and a homoclinic bifurcation at the low bias side. This type is not uncommon in (passive Q-switching) self-pulsating lasers with saturable absorbers [17–21].

V. CONCLUSIONS

We have investigated, both experimentally and theoretically, the dependence of the selfpulsation frequency of semiconductor CD lasers upon changes in the bias current. A distinct kink is found in this dependence, which is investigated using a rate—equation model. We have identified that the kink is caused by spontaneous emission, whose average intensity sets a lower bound on the emitted laser intensity and thereby on the average intensity, which determines the relaxation oscillation frequency.

From our analysis we conclude that below the crossover point, the self-pulsations behave as passive Q-switching oscillations while above the crossover the behavior approaches undamped relaxation oscillations.

The relationship between the relaxation oscillation frequency and the self-pulsation frequency is investigated by means of a small signal analysis. We observe that the relaxation oscillation frequency so obtained is an upper limit for the self-pulsating frequency. It is also

found that self-pulsation occurs in a bias current interval bounded by two Hopf bifurcations. A small window of stable CW emission is found very close to the laser threshold in the absence of spontaneous emission. The model of Ref. [5] does not show such a window of stable emission terminated by a Hopf bifurcation, but a homoclinic bifurcation is responsible for the onset of the self-pulsating behavior. However, for the lasers we used in the experiment, such differences between the models are irrelevant since they occur in a very small range of currents too close to threshold to be resolved. These results raise an interesting question on the nature of the bifurcation at the lower side of the self-pulsation interval.

Note added: A bifurcation analysis of the Yamada model neglecting interstripe diffusion has been published [23]. The bifurcation scenario is different from the one for our model (1a)-(1c) (and closer to the one in [5]). However, these differences in the deterministic behavior have no physical relevance, since they appear in parameter domains for which the dynamics is dominated by noise.

ACKNOWLEDGMENTS

This work was supported by the European Union through the Project HCM CHRX-CT94-0594.

REFERENCES

- [1] N. G. Basov, "Dynamics of injection lasers," IEEE J. Quantum Electron., vol. QE-4, pp. 855–867, 1968.
- [2] R. W. Dixon and W. B. Joyce, "A possible model for sustained oscillations (pulsations) in (Al,Ga)As double-heterostructure lasers", IEEE J. Quantum Electron., vol. QE-15, pp. 470–474, 1979.
- [3] M. Yamada, "A theoretical analysis of self-sustained pulsation phenomena in narrow-stripe semiconductor lasers," *IEEE J. Quantum Electron.*, vol. **29**, pp. 1330–1336, 1993.
- [4] T. Tanaka and T. Kajimura, "Frequency control of self-sustained pulsating laser diodes by uniform impurity doping into multiple-quantum-well structures," *IEEE Photon. Technol. Lett.*, vol. 10, pp. 48–50, 1998.
- [5] G. H. M. van Tartwijk and M. San Miguel, "Optical feedback on self-pulsating semi-conductor lasers," *IEEE J. Quantum Electron.*, vol. **32**, pp. 1191–1202, 1996.
- [6] T. L. Paoli, "Saturable absorption effects in the self-pulsing (AlGa)As junction laser," Appl. Phys. Lett., vol. 34, pp. 652–655, 1979.
- [7] M. Ueno and R. Lang, "Conditions for self-sustained pulsation and bistability in semi-conductor lasers," *J. Appl. Phys.*, vol. **58**, pp. 1689–1692, 1985.
- [8] M. J. Adams and C. Sinthanayothin, "Large-Signal Analysis of Self-Pulsating Laser Diodes", SPIE Proc. vol. 2994, pp. 513-519, (1998).
- [9] E. A. Avrutin, "Analysis of spontaneous emission and noise in self-pulsing laser diodes," *IEE proc. J, Optoelectron.*, vol. **140**, pp. 16–20, 1993.
- [10] U. Bandelow, H.-J. Wünsche, and H. Wenzel, "Theory of self-pulsations in two-section DFB lasers," *IEEE Photon. Technol. Lett.*, vol. 5, pp. 1176-1179, 1993.
- [11] H. Wenzel, U. Bandelow, H.-J. Wünsche, and J. Rehberg, "Mechanisms of fast self-

- pulsations in two-section DFB lasers," *IEEE J. Quantum Electron.*, vol. **32**, pp. 69-78, 1996.
- [12] U. Bandelow, H.-J, Wünsche, B. Sartorius, and M. Mohrle, "Dispersive self-Q-switching in DFB lasers-theory versus experiment," *IEEE J. Sel. Top. Quantum Electron.*, vol. 3, pp. 270-278, 1997.
- [13] P. Phelan, D. McDonald, A. Egan, J. Hegarty, R. O'Dowd, G. Farrell, S. Lindgren, "Comparison of self-pulsation in multisection lasers with distributed feedback and intracavity saturable absorbers," *IEE-Proc. Optoelectron.*, vol. 141, pp. 114–118, 1994.
- [14] A. Egan, J. O'Gorman, P. Rees, G. Farrell, J. Hegarty, and P. Phelan, "Frequency dependence of phase synchronised self-pulsating laser emission and injected periodic electrical signals," *Electron. Lett.*, vol. 31, pp. 802–803, 1995.
- [15] C. H. Henry, "Theory of the linewidth of semiconductor lasers," *IEEE J. Quantum Electron.*, vol. **QE-18**, pp. 259–264, 1982.
- [16] G. H. M. van Tartwijk and D. Lenstra, "Semiconductor laser dynamics with optical injection and feedback," *Quantum Semiclass. Opt.*, vol. 7, pp. 87–143, 1995.
- [17] L. A. Lugiato, P. Mandel, S. T. Dembinski, and A. Kossakowski, "Semiclassical and quantum theories of bistability in lasers containing saturable absorbers," *Phys. Rev. A*, vol. 18, pp. 238–254, 1978.
- [18] T. Erneux , "Q-Switching bifurcation in a Laser with a Saturable Absorber" J. Opt. Soc. Am. B, vol. 5, pp. 1063–1069, 1988.
- [19] E. Arimondo, P. Bootz, P. Glorieux, and E. Meuchi, "Pulse shape and phase diagram in the passive Q switching of CO₂ lasers," *J. Opt. Soc. Am. B*, vol. **2**, pp. 193–201, 1985.
- [20] F. de Tomasi, D. Hennequin, B. Zambon, and E. Arimondo, "Instabilities and chaos in an infrared laser with saturable absorber: experiments and vibrorotational model," J.

- Opt. Soc. Am. B, vol. 6, pp. 45–57, 1989.
- [21] D. Hennequin, F. de Tomasi, L. Fronzoni, B. Zambon, and E. Arimondo, "Influence of noise on the quasi-homoclinic behavior of a laser with saturable absorber," Opt. Comm., vol. 70, pp. 253–258, 1989.
- [22] G. P. Agrawal and N. K. Dutta, Long-wavelength semiconductor lasers, Van Nostrand Reinhold, New York, 1986.
- [23] J.L.A. Dubbeldam, B. Krauskopf, Self-pulsations of lasers with saturable absorber: dynamics and bifurcations, Opt. Comm., vol. 159, pp. 325–338, 1999.

TABLES

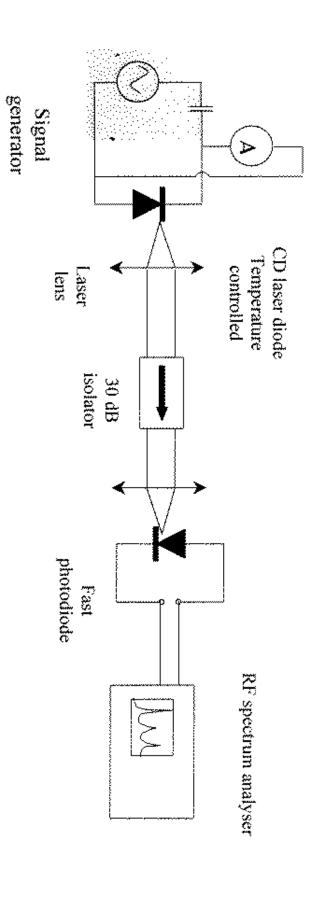
TABLE I. Meanings and values of the parameters in the rate equations

Parameter	Meaning	Value	Units
g_1	Gain parameter of active region	4.7×10^{-9}	ps^{-1}
g_2	Gain parameter of absorbing region	1.5×10^{-8}	ps^{-1}
κ	Inverse photon lifetime	0.4	ps^{-1}
$ au_s$	Carrier lifetime	1.1	ns
eta_{sp}	Spontaneous emission coefficient	variable	dimensionless
η_{sp}	Spontaneous quantum efficiency	0.33	dimensionless
N_{t1}	Carrier number at transparency (active region)	6. 10^7	dimensionless
N_{t2}	Carrier number at transparency (absorbing region)	$1.2 \ 10^8$	dimensionless
J_{th}	Threshold current of the solitary laser	44.53	mA
α	Linewidth enhancement factor	5	dimensionless
v	Ratio of the active and absorbing volumes	0.115	dimensionless
T_{12}	Diffusion time	2.1	ns

FIGURES

FIG. 1. Experimental set-up.

- FIG. 2. Experimentally observed bias current dependence of the emitted laser power (solid line) and the self-pulsating frequency (plus signs).
- FIG. 3. Self-Pulsating Frequency (SPF) vs. Bias Current, obtained by numerically solving Eqs. (1a-1c). The solid line indicates the value of the relaxation oscillation obtained from the small signal analysis. Long-dashed line: SPF in the absence of noise; dash-dotted line: SPF with $\beta_{sp} = 1.3 \times 10^{-4}$; short-dashed line: SPF with $\beta_{sp} = 1.3 \times 10^{-6}$; and dashed-triple-dotted line: $\beta_{sp} = 1.3 \times 10^{-8}$.
- FIG. 4. Time traces of the intensity as a function of the bias current: a) J=45 mA, b) J=80 mA, c) J=84 mA. $\beta_{sp}=1.3\times10^{-6}$
- FIG. 5. Self pulsating frequency (top a)), maximum pulse intensity S_{max} (middle b))and minimum interpulse intensity S_{min} (bottom c)) vs. bias current for $\beta_{sp} = 1.3 \times 10^{-6}$.
- FIG. 6. The real part λ_r of the larger characteristic exponent of the CW solution with positive intensity as a function of bias current. The inset, where the real part of all eigenvalues is included, shows the tiny window of stable CW emission just after threshold.
- FIG. 7. The intensity of the three CW solutions as a function of bias current, when the carrier dependence of the carrier lifetime is included.



Collected Optical Power (mW)

